



HAL
open science

Coherence of particulate beam attenuation and backscattering coefficients in diverse open ocean environments

Toby Westberry, Giorgio Dall'olmo, Emmanuel Boss, Michael Behrenfeld,
Thierry Moutin

► To cite this version:

Toby Westberry, Giorgio Dall'olmo, Emmanuel Boss, Michael Behrenfeld, Thierry Moutin. Coherence of particulate beam attenuation and backscattering coefficients in diverse open ocean environments. *Optics Express*, 2010, 18 (15), pp.15419. 10.1364/OE.18.015419 . hal-02163883

HAL Id: hal-02163883

<https://hal.science/hal-02163883>

Submitted on 29 Dec 2023

HAL is a multi-disciplinary open access archive for the deposit and dissemination of scientific research documents, whether they are published or not. The documents may come from teaching and research institutions in France or abroad, or from public or private research centers.

L'archive ouverte pluridisciplinaire **HAL**, est destinée au dépôt et à la diffusion de documents scientifiques de niveau recherche, publiés ou non, émanant des établissements d'enseignement et de recherche français ou étrangers, des laboratoires publics ou privés.



Distributed under a Creative Commons Attribution 4.0 International License

Coherence of particulate beam attenuation and backscattering coefficients in diverse open ocean environments

Toby K. Westberry,^{1,*} Giorgio Dall'Olmo,¹ Emmanuel Boss,² Michael J. Behrenfeld,¹ and Thierry Moutin³

¹Department of Botany and Plant Pathology, Oregon State University, Corvallis, OR, 97331, USA

²School of Marine Sciences, University of Maine, Orono, ME, 04469-5706, USA

³Laboratoire d'Océanographie Physique et Biogéochimique, UMR 6535 CNRS, Centre d'Océanologie de Marseille, Aix Marseille Université, France

*toby.westberry@science.oregonstate.edu

Abstract: We present an extensive data set of particle attenuation (c_p), backscattering (b_{bp}), and chlorophyll concentration (Chl) from a diverse set of open ocean environments. A consistent observation in the data set is the strong coherence between c_p and b_{bp} and the resulting constancy of the backscattering ratio (0.010 ± 0.002). The strong covariability between c_p and b_{bp} must be rooted in one or both of two explanations, 1) the size distribution of particles in the ocean is remarkably conserved and particle types responsible for c_p and b_{bp} covary, 2) the same particle types exert influence on both quantities. Therefore, existing relationships between c_p or $Chl:c_p$ and phytoplankton biomass and physiological indices can be conceptually extended to the use of b_{bp} . This finding lends support to use of satellite-derived Chl and b_{bp} for investigation of phytoplankton biomass and physiology and broadens the applications of existing ocean color retrievals.

©2010 Optical Society of America

OCIS codes: (010.4450) Oceanic optics; (290.5820) Scattering measurements; (010.1350) Backscattering; (290.5850) Scattering, particles.

References and links

1. H. R. Gordon, and A. Morel, *Remote assessment of ocean color for interpretation of satellite visible imagery. a review* (Springer-Verlag, New York, 1983).
2. H. R. Gordon, O. B. Brown, R. H. Evans, J. W. Brown, R. C. Smith, K. S. Baker, and D. K. Clark, "A semianalytic radiance model of ocean color," *J. Geophys. Res.* **93**(D9), 10909–10924 (1988).
3. S. Maritorena, D. A. Siegel, and A. R. Peterson, "Optimization of a semianalytical ocean color model for global-scale applications," *Appl. Opt.* **41**(15), 2705–2714 (2002).
4. Z. P. Lee, K. L. Carder, and R. A. Arnone, "Deriving inherent optical properties from water color: a multiband quasi-analytical algorithm for optically deep waters," *Appl. Opt.* **41**(27), 5755–5772 (2002).
5. A. Morel, and Y. H. Ahn, "Optics of heterotrophic nanoflagellates and ciliates - a tentative assessment of their scattering role in oceanic waters compared to those of bacterial and algal cells," *J. Mar. Res.* **49**(1), 177–202 (1991).
6. D. Stramski, and D. A. Kiefer, "Light scattering by microorganisms in the open ocean," *Prog. Oceanogr.* **28**(4), 343–383 (1991).
7. M. D. Durand, and R. J. Olson, "Contributions of phytoplankton light scattering and cell concentration changes to diel variations in beam attenuation in the equatorial Pacific from flow cytometric measurements of pico-, ultra- and nanoplankton," *Deep Sea Res. Part II Top. Stud. Oceanogr.* **43**(4-6), 891–906 (1996).
8. R. E. Green, H. M. Sosik, and R. J. Olson, "Contributions of phytoplankton and other particles to inherent optical properties in New England continental shelf waters," *Limnol. Oceanogr.* **48**, 2377–2391 (2003).
9. M. J. Behrenfeld, and E. Boss, "The beam attenuation to chlorophyll ratio: an optical index of phytoplankton physiology in the surface ocean?" *Deep Sea Res. Part I Oceanogr. Res. Pap.* **50**(12), 1537–1549 (2003).
10. M. J. Behrenfeld, and E. Boss, "Beam attenuation and chlorophyll concentration as alternative optical indices of phytoplankton biomass," *J. Mar. Res.* **64**(3), 431–451 (2006).
11. D. Stramski, E. Boss, D. Bogucki, and K. J. Voss, "The role of seawater constituents in light backscattering in the ocean," *Prog. Oceanogr.* **61**(1), 27–56 (2004).
12. G. Dall'Olmo, T. K. Westberry, M. J. Behrenfeld, E. Boss, and W. H. Slade, "Significant contribution of large particles to optical backscattering in the open ocean," *Biogeosciences* **6**(6), 947–967 (2009).

13. M. J. Behrenfeld, E. Boss, D. A. Siegel, and D. M. Shea, "Carbon-based ocean productivity and phytoplankton physiology from space," *Global Biogeochem. Cycles* **19**(1), GB1006 (2005), doi:10.1029/2004GB002299.
14. T. Westberry, M. J. Behrenfeld, D. A. Siegel, and E. Boss, "Carbon-based primary productivity modeling with vertically resolved photoacclimation," *Global Biogeochem. Cycles* **22**(2), GB2024 (2008), doi:10.1029/2007GB003078.
15. J. C. Kitchen, and J. R. V. Zaneveld, "A three-layered sphere model of the optical properties of phytoplankton," *Limnol. Oceanogr.* **37**(8), 1680–1690 (1992).
16. A. L. Whitmire, E. Boss, T. J. Cowles, and W. S. Pegau, "Spectral variability of the particulate backscattering ratio," *Opt. Express* **15**(11), 7019–7031 (2007).
17. D. Stramski, R. A. Reynolds, M. Babin, S. Kaczmarek, M. R. Lewis, R. Rottgers, A. Sciandra, M. Stramska, M. S. Twardowski, B. A. Franz, and H. Claustre, "Relationships between the surface concentration of particulate organic carbon and optical properties in the eastern South Pacific and eastern Atlantic Oceans," *Biogeosciences* **5**(1), 171–201 (2008).
18. E. S. Boss, R. Collier, G. Larson, K. Fennel, and W. S. Pegau, "Measurements of spectral optical properties and their relation to biogeochemical variables and processes in Crater Lake, Crater Lake National Park, OR," *Hydrobiologia* **574**(1), 149–159 (2007).
19. H. Loisel, and A. Morel, "Light Scattering and Chlorophyll Concentration in Case 1 Waters: a Reexamination," *Limnol. Oceanogr.* **43**(5), 847–858 (1998).
20. Y. Huot, A. Morel, M. S. Twardowski, D. Stramski, and R. A. Reynolds, "Particle optical backscattering along a chlorophyll gradient in the upper layer of the eastern South Pacific Ocean," *Biogeosciences* **5**(2), 495–507 (2008).
21. A. Morel, and S. Maritorena, "Bio-optical properties of oceanic waters: a reappraisal," *J. Geophys. Res., [Oceans]* **106**(C4), 7163–7180 (2001).
22. I. Michael, Sieracki, Bigelow Laboratory for Ocean Sciences, 180 McKown Point Road, West Boothbay Harbor, ME, 04575–0475, (personal communication, 2008).
23. W. M. Balch, H. R. Gordon, B. C. Bowler, D. T. Drapeau, and E. S. Booth, "Calcium carbonate measurements in the surface global ocean based on Moderate-Resolution Imaging Spectroradiometer data," *J. Geophys. Res., [Oceans]* **110**(C7), C07001 (2005).
24. H. Loisel, J. M. Nicolas, A. Sciandra, D. Stramski, and A. Poteau, "Spectral dependency of optical backscattering by marine particles from satellite remote sensing of the global ocean," *J. Geophys. Res., [Oceans]* **111**(C9), C09024 (2006).
25. T. S. Kostadinov, D. A. Siegel, and S. Maritorena, "Retrieval of the particle size distribution from satellite ocean color observations," *J. Geophys. Res., [Oceans]* **114**(C9), C09015 (2009).
26. M. S. Twardowski, E. Boss, J. B. Macdonald, W. S. Pegau, A. H. Barnard, and J. R. V. Zaneveld, "A model for estimating bulk refractive index from the optical backscattering ratio and the implications for understanding particle composition in case i and case ii waters," *J. Geophys. Res., [Oceans]* **106**(C7), 14129–14142 (2001).
27. E. Boss, W. S. Pegau, M. Lee, M. Twardowski, E. Shybanov, G. Korotaev, and F. Baratange, "Particulate backscattering ratio at LEO 15 and its use to study particle composition and distribution," *J. Geophys. Res., [Oceans]* **109**(C1), C01014 (2004).
28. R. A. Meyer, "Light scattering from biological cells: dependence of backscatter radiation on membrane thickness and refractive index," *Appl. Opt.* **18**(5), 585–588 (1979).

1. Introduction

Ocean color satellites measure the water leaving radiance originating from a thin layer just beneath the surface of the ocean, which is analytically and empirically related to the absorbing and scattering constituents contained therein [1,2]. Thus, *in situ* measurements of absorption and scattering are critical for developing and validating models relating satellite measurements to in-water optical properties, and consequently, the biogeochemical processes which affect them.

The particulate scattering coefficient (b_p) quantifies the intensity of total scattered light (neglecting water) and is composed of a large forward component and a small (~1%) backward component (b_{bp}) which contributes to satellite reflectance measurements [3,4]. These two scattering indices have been theoretically linked to two distinct types of particles, predominantly distinguished by their size. Small (<1 μ m) non-living particles are thought to determine the magnitude of backscattering based on Mie theory calculations, while larger (~0.5–20 μ m) particles preferentially affect the forward scattering [5,6]. This larger size fraction overlaps the size domain of most phytoplankton in the ocean and evidence has been presented which relates b_p (or nearly equivalently, c_p , the particulate beam attenuation coefficient) to phytoplankton biomass and physiology [7–10]. On the other hand, no *direct* evidence exists supporting the relationship between b_{bp} and the sub-micron particle pool, due to experimental difficulties measuring the latter. Nevertheless, it is routinely accepted that these small particles greatly influence b_{bp} (but see [11,12]).

Recently, other investigators have proposed that b_{bp} can instead, be related directly to phytoplankton biomass [13,14]. This proposition should be valid under at least two different scenarios, (1) phytoplankton directly contribute a significant fraction of b_{bp} in addition to, or instead of, the presumed sub-micron particle assemblage and/or (2) small and large particles strongly covary in the open ocean. Towards this end, recent evidence suggests phytoplankton may in fact contribute more to b_{bp} than is currently apportioned based on Mie theory alone [12]. Modeling studies incorporating more detailed descriptions of phytoplankton morphology and internal structure also share this finding [15] and in a recent review of backscattering in the ocean, Stramski et al. [11] clearly document theoretical shortcomings in explaining existing observational data sets. In addition, reports that the $b_{bp}:b_p$ ratio is relatively constant across diverse oceanic environments [16,17] are becoming more widespread with the advent of easy-to-use commercially available backscattering meters. Despite these findings, reluctance towards using b_{bp} to study phytoplankton has been strong, due to the prevailing paradigm suggesting that “small, non-living” particles determine the magnitude of backscattering in the open ocean.

The objective of this work is to investigate the covariability between c_p and b_{bp} in different regions of the global *open* ocean based on extensive shipboard data collected in diverse environments. We compare and contrast our data with existing results in the literature and show a consistent, quantitative relationship between the two scattering indices and between regions.

2. Methods

All of the *in situ* data presented here were collected during four cruises to the Equatorial Pacific (April-May 2007, *R/V Ka'imi Moana*), North Atlantic (May 2008, *R/V Knorr*), Mediterranean Sea (June-July 2008, *R/V L'Atalante*), and Subarctic Northeast Pacific (August 2009, *CCGS John P. Tully*) totaling ~75 measurement days. Digital measurements were collected with the same experimental setup on all four cruises using the ship's clean water supply in a quasi-continuous manner. In addition, periodic comparisons were made between this “flow-through” water source and surface seawater collected with a traditional CTD rosette for validation (see Discussion). Subsequent data processing of optical measurements was also consistent between the four cruises, thus minimizing or eliminating methodological differences.

Bio-optical data were collected with a suite of instruments including a hyperspectral absorption-attenuation meter (ACs), multispectral backscattering sensor (ECO-BB3), and 2 single wavelength C-Star transmissometers (526 & 660 nm). Prior to interrogation by the instruments, surface seawater was passed through 2 consecutive vortex debubblers and an electronically actuated valve programmed to divert seawater flow through a 0.2 μm nylon cartridge filter for 10 minutes each hour. For the remaining 50 minutes of each hour, seawater flow was uninterrupted and constitutes “bulk” measurements. Piecewise linear interpolation of the 0.2 μm filtered periods provides a baseline primarily representing “dissolved” substances, but also including calibration uncertainties and short term bio-fouling. Subtraction of the baseline from bulk absorption and attenuation measurements yields calibration independent *particulate* optical quantities, with uncertainties at the level of instrument precision [12,18].

All subsequent processing of AC-s, C-Star, and ECO-BB3 data followed procedures described in [12]. Particulate backscattering, $b_{bp}(\lambda)$, was measured reliably at two wavelengths (470 and 526 nm), but in the current analyses, we report measurements at a single wavelength, 526 nm, as results at other wavelengths are similar.

3. Results

Chlorophyll concentrations varied over three orders of magnitude across data sets from extremely oligotrophic (<0.05 mg m^{-3}) to mesotrophic (~5 mg m^{-3}). Total particulate attenuation at 526 nm, $c_p(526)$, ranged from <0.05 to 1 m^{-1} , while particulate backscattering, $b_{bp}(526)$, ranged from 0.0004 to 0.01 m^{-1} . On average, particulate absorption at 526 nm,

$a_p(526)$, was a near-negligible fraction of $c_p(526)$ ($\sim 4 \pm 1\%$), such that $c_p \approx b_p$. This is true across most of the visible spectrum, except near the phytoplankton absorption maximum in the blue (~ 440 nm) and is noteworthy for comparison with historical relationships which may use b_p or c_p , whereas we will consider them equivalent (see also [19]). Figure 1A shows $b_{bp}(526)$ plotted versus $c_p(526)$ for the four cruises. The number of data points ($N \sim 10^5$) requires a bivariate histogram to see underlying trends. A weighted linear least squares regression applied to all data yields a slope of $(9.1 \pm 0.4) \times 10^{-3}$ and an intercept of $(2.0 \pm 0.1) \times 10^{-4} \text{ m}^{-1}$ ($r^2 = 0.92$, uncertainties estimated from 1000 bootstrap samples). The resulting backscattering ratios (dimensionless) are shown in Fig. 1B and can be described by a median value \pm the percentile range equivalent to a standard deviation around a normal distribution. For the Equatorial Pacific, North Atlantic, Mediterranean Sea, and Northeast Pacific these values are 0.011 ± 0.001 , 0.010 ± 0.002 , 0.010 ± 0.002 , and 0.012 ± 0.003 respectively. The full range of the four data sets, described by the 5th-95th percentile range, is 0.007-0.015.

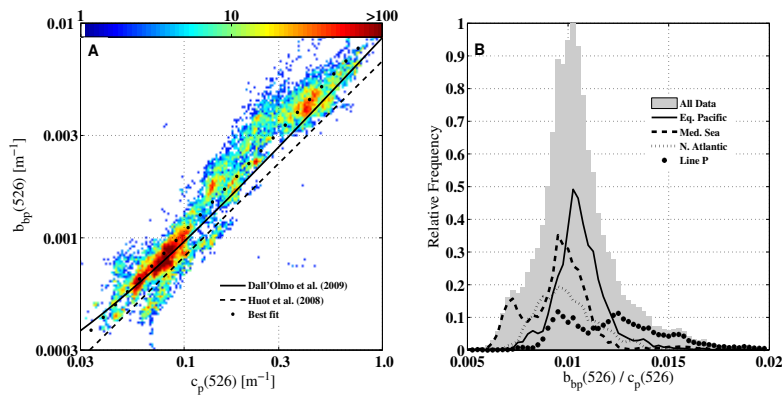


Fig. 1. **A.** Relationship between backscattering (b_{bp}) and beam attenuation (c_p) at 526 nm (colors indicate number of observations at each b_{bp}, c_p pair). “Best fit” line is calculated from weighted linear regression of 2D histogram with weights assigned as the square of the number of points found in each bin. Relationship of Huot et al. [20] (dashed line) was derived from equivalence of their Eqs. (8) and 9, while that of Dall’Olmo et al. [12] (solid line) was derived from the Equatorial Pacific data set alone. **B.** Distributions of backscattering ratio ($b_{bp}: c_p$) at 526 nm for each data set and for all data combined. Histograms have been normalized to the total number of observations ($N \sim 10^5$).

Figures 2A and 2C show the two scattering indices, c_p and b_{bp} , as a function of chlorophyll concentration. Particle attenuation (c_p) and scattering (b_p) have been empirically related to Chl for a long time and several relationships can be found in the literature [19–21]. The typical open ocean standard is taken from [19] which provided expressions for different vertical layers, and for a few different regions of the ocean (e.g., the North Atlantic). Data presented here match the expected values of c_p from [19] at low Chl , but deviate significantly at higher Chl , which in our data set come almost exclusively from the North Atlantic. However, the fit derived by Loisel and Morel [19] when their own North Atlantic data were included is in good agreement with data presented here (normalized median bias (NMB), $X_{\text{measured}} - X_{\text{modeled}} / X_{\text{measured}} * 100 \sim 11\%$, consistent with the difference in acceptance angles of the instruments used in the two studies). Loisel and Morel [19] assumed that this increased scattering per unit chlorophyll observed when the North Atlantic data were included was due to the presence of coccolithophorids and/or detached liths. On the contrary, in our data set, coccolithophorids and their liths were not observed in flow cytometric and microscopic measurements [22]. Also, the backscattering ratio, which was unavailable to Loisel and Morel [19], is not significantly higher in the North Atlantic data presented here than in the other data sets (Fig. 1B). The backscattering of coccolithophorids and their liths is a hallmark of their presence and is the basis for their detection in satellite ocean color data [23].

Similarly, $b_{bp}(526)$ from the North Atlantic is significantly higher than expected based on the relationships of Morel and Maritorena [21], while agreement improves at lower chlorophyll concentrations (Fig. 2C). The updated relationship of Huot et al. [20] also agrees better at lower Chl , but still underestimates our observations of $b_{bp}(526)$ at moderate to high chlorophyll concentrations (normalized median difference = 42% when $Chl > 1 \text{ mg m}^{-3}$). It is these higher values for which we have direct validation (see Discussion and Fig. 3C) and therefore, disagreement with previously published relationships in the high Chl range (1-10 mg m^{-3}) may be related to the paucity of high Chl open ocean observations in previous data sets rather than uniqueness in the data presented here.

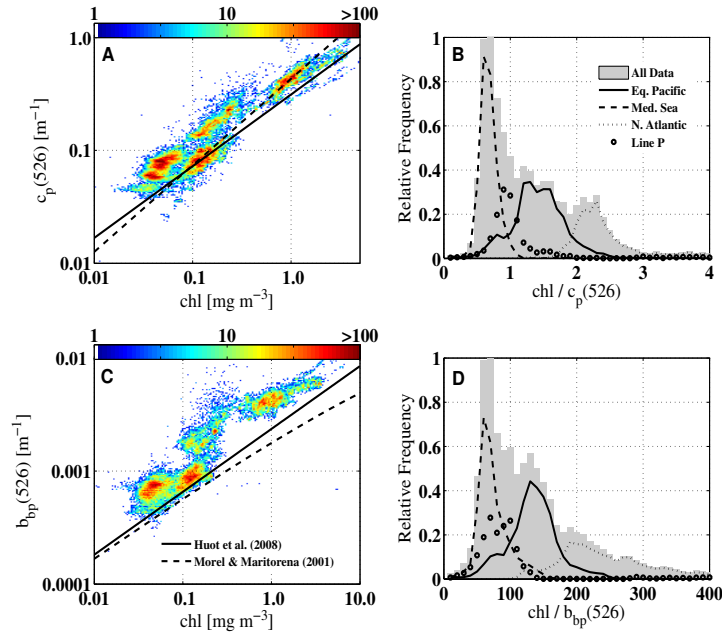


Fig. 2. Particle beam attenuation (c_p) and backscattering (b_{bp}) at 526 nm as a function of chlorophyll (Chl). Chl (mg m^{-3}) is estimated using an absorption line height approach [18] where $Chl = (a_p(676) - (0.6a_p(650) + 0.4a_p(714))) / a^*_{Chl}$ and $a^*_{Chl} = 0.014 \text{ m}^2 \text{ mg}^{-1}$; **A**, $c_p(526)$ versus Chl . Solid black line is the model of Loisel and Morel [19], dashed black line is [19] when including their North Atlantic data. Loisel and Morel [19] relationships were extrapolated to 526 nm (from 660 nm) using a spectral slope of λ^{-1} ; **B**, distribution of the ratio $Chl:c_p$ for each cruise and all data combined; **C**, $b_{bp}(526)$ versus Chl . Solid black line is the model of Huot et al. and dashed black line is model of Morel and Maritorena [21]; **D**, distribution of the ratio $Chl:b_{bp}$ for each cruise and all data combined.

4. Discussion

The accuracy and precision of the measurements presented here can be evaluated with a limited number of overlapping measurements for chl , c_p , and b_{bp} . Discrete matchups with HPLC-derived Chl are in excellent agreement (Fig. 3A), median bias in ACs-based Chl estimates is $-0.002 \pm 0.067 \text{ mg m}^{-3}$ (NMB = $-2\% \pm 18\%$). Similar matchups of c_p with transmissometers mounted on the CTDs of each cruise also compare well, median bias is $0.0001 \pm 0.031 \text{ m}^{-1}$ (NMB = $-0.2\% \pm 11.4\%$) (Fig. 3B). Comparisons with independent b_{bp} estimates were only available for the subset of data taken from the North Atlantic and are shown in Fig. 3C. One caveat is that the sensors, although identical, measured at different wavelengths (526 and 700 nm for the underway and CTD-mounted instruments, respectively) and it might be expected *a priori* that b_{bp} values be slightly higher at 526 nm than 700 nm depending upon the slope of the backscattering spectrum. However, in highly productive

regions such as the North Atlantic, we can expect the backscattering spectrum to be relatively flat (slope \sim 0, e.g., [24,25]) and spectral differences to be minimal. The median ratio of the underway to CTD b_{bp} values is 1.04 ± 0.07 suggesting that underway b_{bp} values are \sim 4% higher. Thus, the values we present are robust and have no significant biases.

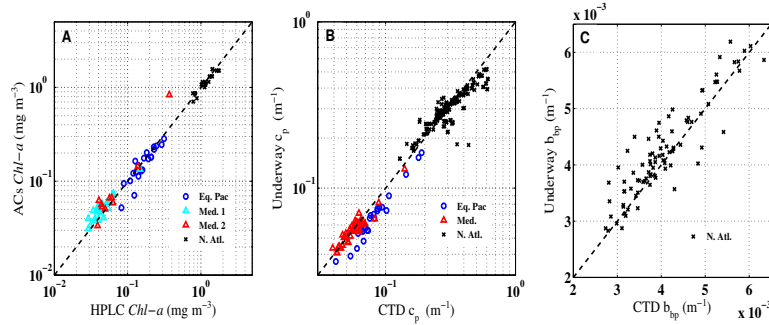


Fig. 3. Chlorophyll (Chl), particle attenuation (c_p) and backscattering (b_{bp}) matchups between continuous flow through measurements and discrete *in situ* measurements. **A.** HPLC total $Chl-a$ ($Chl a + divinyl Chl a + Chlorophyllide a$) plotted versus simultaneous AC-s estimates made using absorption line height method (see previous figure caption). $N = 99$, $r^2 = 0.94$. **B.** Near surface c_p (depth < 5 meters) calculated from CTD-mounted instruments on each cruise plotted versus simultaneous measurements with similar instrument (WETLabs C-Star, 660nm) made on continuous flowing seawater from ship's intake. $N = 262$, $r^2 = 0.91$. **C.** CTD-mounted b_{bp} estimates (depth < 5 m) versus underway estimates, $N = 89$, $r^2 = 0.83$. Dashed line in each represents 1:1 line.

Most studies of the backscattering ratio to date have focused on contrasting the full range of $b_{bp}:c_p$ from surface open ocean to coastal waters to bottom boundary layers [16,26,27]. Huot et al. [20] reported the first comprehensive set of b_p , b_{bp} , and Chl measurements in the open ocean and found a median $b_{bp}:c_p$ at 532nm \sim 0.006 with no obvious Chl dependence. However, the same quantity at neighboring wavelengths (510 and 589 nm) was also measured by [17] and found to be higher ($b_{bp}:c_p \sim$ 0.01). Here we greatly expand the range, both dynamic and geographic, and number of measurements ($N \sim 10^5$ compared to $N \sim 10^2$) to examine the robustness of these findings. While our conclusions are somewhat similar, we find a median value ($b_{bp}:c_p \sim$ 0.01) which is remarkably conserved across very different oceanic environments and in good agreement with Stramski et al. [17] and Whitmire et al [16]. Although it is impossible to determine the exact reason for this observation with current data, one intriguing hypothesis is that phytoplankton-sized particles contribute significantly to both c_p and b_{bp} [10,12]. Indeed, for much of the ocean, c_p variability reflects phytoplankton biomass [9,10]. Given the universal coherence between c_p and b_{bp} found here, it would appear that b_{bp} conveys similar information. Arguments against this possibility rely on [Mie] theoretical results which have documented shortcomings in their treatment of phytoplankton attributes [28]. Nevertheless, if this observation holds true, utilization of b_{bp} as a proxy for phytoplankton biomass and the $Chl:b_{bp}$ ratio as a phytoplankton physiological index should be possible [13,14].

One point of departure between these data and those previously reported (e.g., [19,20]) is the seemingly poor relationship between Chl and c_p or b_{bp} . This is in contrast to the usual presumption that the two scattering indices smoothly vary as a function of Chl , albeit with some degree of noise (c.f., large amount of scatter in Fig. 3A of [19]). Although the first order dependence is indeed due to biomass (and thus Chl by association), there are several reasons to expect significant dispersion in either of these relationships. Differences in cell size, photoacclimation state, and nutrient limitation (particularly with respect to iron) will all exert control on cellular chlorophyll content, and thus, the apparent chlorophyll per unit scattering (or backscattering). The collective data set presented here spans a large gradient in each of these factors and a simple qualitative accounting due to each provides insight to the individual $Chl:c_p$ distributions seen in Fig. 2B. For example, the oligotrophic Mediterranean Sea data can

be characterized as *Synechococcus* and *Prochlorococcus* dominated (from HPLC data, not shown) which are high-light and low-nutrient acclimated. The small size of these phytoplankters (cell diameter $\leq 1\mu\text{m}$) and their subtropical, high light environment give them the smallest $Chl:c_p$ ratio (Fig. 2B). In contrast, the springtime North Atlantic data were collected under diatom-rich conditions (HPLC data, not shown) having typical sizes from $\sim 10\mu\text{m}$ to greater than $100\mu\text{m}$. Acclimation irradiances were presumably quite low based on the time of year (May), high latitude ($\sim 62^\circ\text{N}$) and moderately deep mixed layer depths ($\sim 40\text{--}50\text{ m}$, not shown). The combined effects of these growth conditions result in the highest $Chl:c_p$ values observed (Fig. 2B). Last, we know that the Equatorial Pacific and subarctic North Pacific are chronically iron limited regions, while the North Atlantic and Mediterranean are generally not, making iron effects on intracellular *Chl* and growth an important consideration also.

In summary, we show that variance around the $b_{bp}:c_p$ ratio over its entire range is much smaller than that of the $Chl:c_p$ or $Chl:b_{bp}$ ratio, suggesting that the two scattering indices, c_p and b_{bp} , are better related to one another than either are to the traditional pigment biomass index, *Chl*. The quality and unprecedented number of observations reported here gives a fresh view of how these properties are related (or not) to one another. Unfortunately, we do not currently have all the data required to confirm reasons for the coherence of b_{bp} and c_p , nor the variability in $Chl:c_p$ and $Chl:b_{bp}$ ratios. However, expected variability in these ratios due to environmental factors is consistent with their observed distributions. It follows that relationships between c_p and phytoplankton biomass [8], or between $Chl:c_p$ and phytoplankton physiological indices [9], can be conceptually extended to the use of b_{bp} . This finding lends support to the use of satellite-derived *Chl* and b_{bp} for investigation of phytoplankton biomass and physiology and broadens the applications of existing ocean color retrievals. Ongoing validation in different oceanic environments, particularly the oligotrophic subtropical gyres, is nevertheless, desirable.

Acknowledgements

This work was funded by NASA grant number NNX08AK70G and NNG05GD18G. The authors would like to thank Josephine Ras and Mary Jane Perry for providing validation data used in Fig. 3. We would also like to thank the captains, crews, and scientific participants aboard the cruises used in this work. The BOUM cruise in the Mediterranean Sea was co-funded by the French national LEFE-CYBER program (INSU CNRS) and the European IP SESAME.